Nanobiotechnol (2007) 3:96–103
DOI 10.1007/s12030-007-0007-1

Layer-by-layer Assembly of Poly(lactic-*co*-glycolic acid)-*b*-poly(L-lysine) Copolymer Micelles

Eunah Kang · Sang Cheon Lee · Kinam Park

Published online: 17 July 2007

Abstract Biocompatible, biodegradable polyionic micelles were used as a building component for layer-by-layer (LbL) assembly that can produce drug-loaded nanolayers. To prepare the polycationic micelles, poly(lactic-*co*-glycolic acid)-*b*-poly(L-lysine) [PLGA-*b*-P(Lys)] copolymers were synthesized. In an aqueous phase, PLGA-*b*-P(Lys) copolymers were self-assembled to form spherical micelles with the inner core of poly(lactic-co-glycolic acid) (PLGA) and the cationic outer shell of P(Lys). The micelles were characterized by zeta potential, dynamic light scattering, and nuclear magnetic resonance. PLGA-*b*-P(Lys) micelles showed the positive zeta potential values in a broad range of pH (3–11), indicating the high stability of the polyionic micelles with the outer shell of positive charges. Cationic polymeric micelles were coated on the surface via electrostatic interactions with the oppositely charged polyelectrolyte, poly(sodium 4-styrenesulfonate). Formation of multiple micelle layers was monitored using quartz crystal microbalance *in situ*, and the surface topology of the layers was characterized by atomic force microscopy *ex situ*, as the number of micelle layer was increased. The multiple micelle layers were stable, and the thickness of micelle layer grew as the number of LbL coating increased. The approach described in this work can be used for the development of the biocompatible, biodegradable, drug-loaded bioactive nanocoatings.

Keywords layer-by-layer assembly · biocompatible · polymeric micelles · PLGA · poly(L-lysine)

E. Kang · K. Park
Weldon School of Biomedical Engineering, Purdue University, West Lafayette, IN, USA

S. C. Lee
Nanomaterials Application Division, Korea Institute of Ceramic Engineering and Technology,
Seoul 153-801, Republic of Korea

K. Park
Department of Pharmaceutics, Purdue University,
West Lafayette, IN, USA

K. Park (✉)
Department of Biomedical Engineering, Purdue University,
BMED Building, 206 South Intramural Drive,
West Lafayette, IN 47907, USA
e-mail: kpark@purdue.edu

Introduction

Polymeric micelles composed of the hydrophobic core and the hydrophilic corona have been studied extensively in the pharmaceutical area as effective carriers for poorly soluble drugs [1–6]. The successes of polymeric micellar drug delivery systems are attributed to their high drug capsulation efficiency and their ability to release the loaded drug in a controlled manner. Various chemical structures of polymers have been designed to provide additional properties, such as thermo- and pH-sensitivities. Supramolecular lipid vesicles have also been assembled on a solid surface for development of architectural nanomaterials as potential nanodevices [7–13]. Lipid vesicles have been used as building blocks for layer-by-layer (LbL) assembly through electrostatic interactions [8, 14]. It has been noticed, however, that the lipid vesicles embedded within the counterion layers of polyelectrolytes are not stable enough to maintain the hydrophilic reservoir space, resulting in vesicle fusion or rupture [14, 15]. The instability of lipid vesicles within polyelectrolyte-coated layers was improved by the cross-linking of lipids [11, 16, 17]. Lipid vesicle assemblies are only capable of loading hydrophilic mole-

cules, whereas many important drugs are hydrophobic in nature.

Polymeric micelles have been the choice for delivering poorly soluble drugs, such as paclitaxel. Polymeric micelles can also be used as a building block for nanoarchitecture assembly into hierarchically integrated structures [18–20]. Covalent bonding through functionally activated outer end groups of polymeric micelles increases the stability of the assembled multilayers [21–24]. An alternative method of making stable LbL deposition is sequential depositions of polyionic polymeric micelles and polyelectrolytes with the counter charge. LbL deposition through electrostatic interactions has been achieved in various applications, such as coating of poly(styrene-*b*-acrylic acid) micelles onto optic materials [25]. This approach of building polymeric micelle architecture can also be useful for assembling a drug-loaded bioactive layer that can modulate drug release.

This study describes LbL assembly of polyionic micelles constructed from self-assembly of PLGA-*b*-P(Lys). Poly (lactic-*co*-glycolic acid)-*b*-poly(L-lysine) [PLGA-*b*-P(Lys)] copolymer micelles has been applied for drug and gene delivery because of its biocompatible properties [26, 27]. The block combination of PLGA and P(Lys) makes it possible to generate the extremely biocompatible and biodegradable nanocoatings consisting of nanolayers through a LbL approach. The possibility of LbL deposition of PLGA-*b*-P(Lys) micelles on the surface to build three-dimensional polymeric micelle multilayers was examined.

Materials and Methods

Materials

Poly(lactic-*co*-glycolic acid) (PLGA) (50/50) polymers were obtained from Alkermes (Wilmington, OH, USA). Poly(allylamine hydrochloride) (PAH) (M_w 70 K) and poly (sodium 4-styrenesulfonate) (PSS) (M_w 70 K) were purchased from Aldrich (Milwaukee, WI, USA). ε-(Benzyloxycarbonyl)-L-lysine (*Z*-L-lysine) was purchased from Sigma (Milwaukee, WI, USA) and was used as received. Ethylenediamine (EDA), 1,3-dicyclohexylcarbodiimide (DCC), 4-dimethylaminopyridine (DMAP), triphosgene, and HBr/HOAc were purchased from Aldrich and were used without further purification. Tetrahydrofuran (THF) from Aldrich was refluxed and distilled over Na/benzophenone before use. Dimethylformamide (DMF) was dried and distilled under the vacuum using calcium hydride. Chloroform, ethanol, and diethyl ether were of reagent grade.

Synthesis of PLGA-*b*-P(Lys) Block Copolymer [PLGA-*b*-P (Lys)]

Synthesis of the copolymers is briefly described below, and the synthetic scheme of PLGA-*b*-P(Lys) block copolymers is presented in Scheme 1.

N-Carboxyanhydride of ε-(Benzyloxycarbonyl)-l-lysine

ε-(Benzyloxycarbonyl)-L-lysine *N*-carboxyanhydride [Lys (*Z*)-NCA] was synthesized by the procedure reported by Daly and Poche [28]. Lys(*Z*) was suspended in THF at 50° C. Triphosgene was added into the Lys(*Z*)-suspended solution. After 3 h, the product was precipitated into hexane and recrystallized with THF and hexane.

Amine-terminated Poly(lactic-co-glycolic acid)

A solution of PLGA (5 g) in THF (50 ml) was added dropwise to a stirred solution of EDA (0.225 g, 3.8 mmol), DCC (0.774 g, 3.8 mmol), and DMAP (0.046 g, 0.38 mmol) in THF at 25°C. Reaction was maintained for 24 h under nitrogen. Precipitated dicyclohexylurea was filtered off. Amine-terminated PLGA was isolated by repeated precipitation into ethanol and then into diethyl ether.

PLGA-b-P(Lys) Block Copolymer

A solution of PLGA in DMF (10 ml) was then added drop by drop into a solution of Lys(*Z*)-NCA (4.71 g, 0.015 mol)

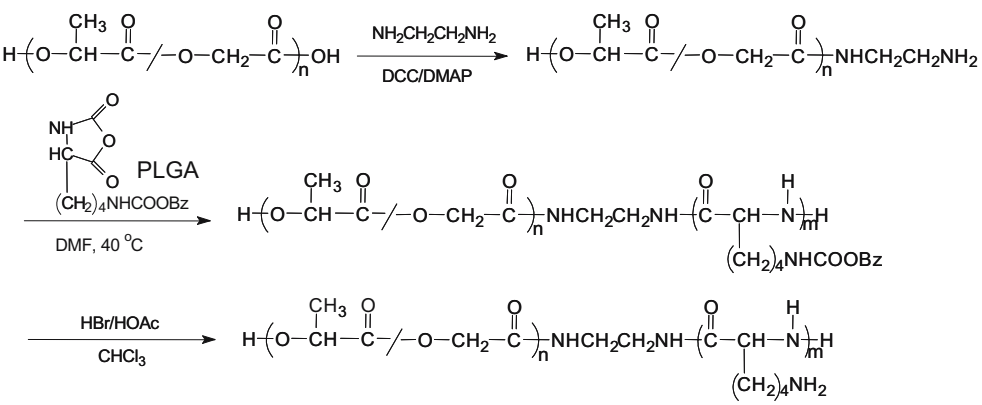

Scheme 1 Synthetic scheme of PLGA-*b*-P(Lys) copolymer

in DMF (40 ml). The reaction mixture was stirred for 24 h at 40 °C under nitrogen. PLGA-*b*-P(Lys(*Z*)) was isolated by repeated precipitation into diethyl ether.

Deprotection of PLGA-b-P(Lys(Z))

A chloroform solution (20 ml) of PLGA-*b*-P(Lys(*Z*)) (1 g) was treated with HBr/HOAc (7 ml) under nitrogen. The reaction mixture was then stirred for 30 min. The crude product was precipitated in diethyl ether and filtered. The precipitate was redissolved in chloroform (15 ml) and neutralized by the treatment with triethylamine (3 ml) for 10 min. The product, PLGA-*b*-P(Lys), was isolated by the precipitation into ethanol and dried at 40 °C under the vacuum.

Characterization of PLGA-*b*-P(Lys) Block Copolymer

Molecular weight and polydispersity of the PLGA-*b*-P(Lys) copolymer were characterized by size exclusion gel permeation chromatography (GPC) (PLgel, 5 μm mixed D column, Polymer Laboratories Inc., Amherst, MA, USA). Agilent LC system combined with the Agilent refractive index detector. THF was used as a mobile phase with a flow rate of 1 ml/min at 40°C. Molecular weights were calculated using polystyrene references (Polymer Laboratories Inc.). The ^{1}H NMR spectra were obtained from an ARX 300 NMR spectrometer at 300 MHz.

Micelle Preparation and Characterization

PLGA-*b*-P(Lys) solution (5 mg/ml in DMSO) was dialyzed against 0.1 M NaCl (pH 6.5) in distilled water for 24 h and lyophilized. The formed PLGA-*b*-P(Lys) micelles were characterized with dynamic light scattering and zeta potentiometer. The size distribution of micelles was estimated from the hydrodynamic diameter using a dynamic light scattering system (Photocor), which was equipped with a He–Ne laser (20 mW, 633 nm). Measurements were taken at 25°C with a detection angle of 90° in duplicate. Zeta potential of PLGA-*b*-P(Lys) micelles was characterized using a Doppler electrophoretic light scattering analyzer (DELSA 440, Coulter). pH of micelle solutions was adjusted from 3 to11 using 10 mM of NaCl or HCl in water. PLGA-*b*-P(Lys) micelles were dispersed with a concentration of 0.1 mg/ml in water.

LbL Coating and Characterization

Glasses were cleaned with piranha solution (70% sulfuric acid and 30% hydrogen peroxide) and water, followed by a drying process under a stream of nitrogen. PAH and PSS were used for a polyelectrolyte LbL coating. Cover glasses were immersed in the 20 mM PAH solution (1.44 mg/ml, 0.1 M NaCl, pH 6.5) for 5–10 min and subsequently immersed in a 20 mM PSS solution (4.1 mg/ml, 0.1 M NaCl, pH 6.5) for 5–10 min [29]. Layered substrates with polyelectrolytes were immersed into 0.12% w/v micelle solution at pH 6.5 for 1 h. Substrates were washed with water (pH 6.5) or 0.1 M NaCl (pH 6.5) between each layering. Coating steps were repeated until the desired number of PLGA-*b*-P(Lys) micelle multilayer was achieved. Layer-deposited substrates were freeze-dried to prevent micelle aggregation during drying.

Mass adsorption of polyelectrolytes and micelles was characterized using *in situ* quartz crystal microbalance (QCM dissipation, Qsense, Sweden). QCM dissipation techniques have been described previously [15, 30]. A silicon(Si/SiO_2) crystal (diameter 14 mm) was oscillated at its fundamental frequency (f_0) of 5 MHz and the change of resonance frequency (Δf) was monitored with the third overtone (n=3), analogous with 15 MHz. The crystal of the Si/SiO_2 surface was cleaned with piranha solution and then placed into a 80-μl measurement chamber. The frequency (f) and dissipation (D) of the crystal were recorded until the signal was equilibrated under atmosphere. Subsequently, 2 ml of 0.1 M NaCl (pH 6.5) was introduced into the chamber via a discontinuous plug flow passing a temperature-controlled loop. Polyelectrolyte solution with an injection volume of 500 μl was added to the chamber at 23°C for 10 min. Two pairs of PAH/PSS film were coated by sequential steps that were monitored by QCM *in situ*. Excess polyelectrolytes solution in each layer formation was removed by exchanging it with 0.1 M NaCl solution. Cationic polymeric micelle dispersion to form the first micelle layer was introduced to the substrate, followed by PSS or PAH film deposition. Similarly, multiple layers of micelles were formed and frequency changes in situ were recorded at the third overtone (N=3).

The adsorption mass was obtained from the Sauerbrey equation that designates a linear relation between the frequency changes (Δf) and the mass per unit area (Δm).

$$\Delta m = -\frac{C\Delta f}{N}$$

where C (17.7 ng cm^{-2} Hz^{1}) is a proportional constant that depends on intrinsic properties of the quartz and N is the overtone number. Surface topology and the thickness of LbL micelle layers were characterized using atomic force microscopy (Nanoscope IIIa (Digital Instruments, CA, USA). Layer-deposited substrates were imaged by a tapping mode and silicon nitride tips with a spring constant of 42 N/m were used. For the thickness measurement, the layer was scratched using a razor (number=9) and images of the scratched area were taken. Line analysis and a depth

profile on the image were carried out, and thickness was measured (n=5).

Results and Discussion

Synthesis of PLGA-*b*-P(Lys) Block Copolymer and Characterization

A block copolymer of PLys and PLGA was synthesized as shown in Scheme 1. PLGA was end-functionalized with a primary amine via a DCC-mediated coupling reaction between the carboxyl group of PLGA and the amine group of EDA. The primary amine group of PLGA was then used to initiate the ring-opening polymerization of Lys(*Z*)-NCA to yield the block copolymer, PLGA-*b*-P(Lys(*Z*)). Deprotection of benzyloxycarbonyl groups resulted in PLGA-*b*-P(Lys) copolymer. The structure and molecular weight were analyzed by ^{1}H NMR spectrum and GPC, respectively. ^{1}H NMR spectra of PLGA-*b*-P(Lys) copolymer and PLGA-*b*-P(Lys(*Z*)) in DMSO-d_6 or D_2O are presented in Fig. 1. The resonance peak at 7.28 ppm was assigned to phenyl photons of the ε-benzyloxycarbonyl group of P(Lys(*Z*)) block (Fig. 1a). The repeating units of lactic acid were peaked at 5.22 and 1.47 ppm. The peaks at 3.3 and 2.9 ppm were assigned to the lysine structure of PLys(*Z*) block. In Fig. 1b, the phenyl resonance peak of the benzyloxycarbonyl group at 7.28 ppm disappeared, which confirmed the deprotection of benzene groups. Thus, Fig. 1b confirms synthesis of PLGA-*b*-P(Lys) copolymer. The degree of polymerization integrated from the number of the monomer unit of P(Lys(*Z*)) block was 15. The GPC trace of the block copolymer showed a monomodal profile (Fig. 2). The number average molecular weight (M_n) and polydispersity index (PDI) of PLGA-*b*-P(Lys(*Z*)) were 22,900 and 1.42, respectively. This result indicated that block copolymerization was successfully completed, and the homopolymer was not included in the obtained final product.

As mentioned above, the ^{1}H NMR spectrum of PLGA-*b*-P(Lys) in DMSO-d_6 showed all proton resonances of both the PLGA block and the P(Lys) block. Unlike the spectrum of PLGA-*b*-P(Lys) in DMSO-d_6, the spectrum measured in D_2O showed only (C**H**) resonance at 4.14 ppm and (C**H**$_2$)$_3$ resonance of P(Lys) block at 1.56 and 1.27 ppm. In contrast, the peaks of 5.19 (methine) and 1.44 (methyl) ppm for the lactic acid unit and the peak of 4.87 ppm for the glycolic acid unit were vanished, as shown in Fig. 1c. This result indicated that the core of PLGA was in a pseudosolid state because NMR spectrophotometer resolved only the solvated status of a molecular structure. Thus, the micelles of PLGA-*b*-P(Lys) were composed of the core of the PLGA block and the outer corona of the P(Lys) block.

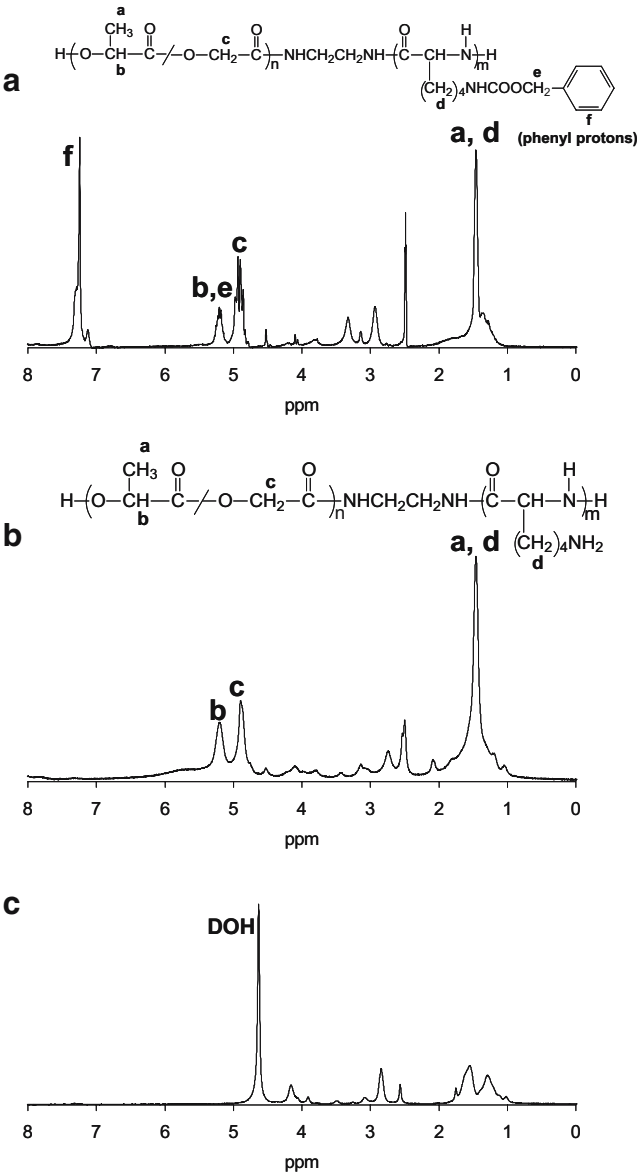

Fig. 1 NMR analysis **a** PLGA-*b*-P(Lys(*Z*)) in DMSO-d_6, **b** PLGA-*b*-P(Lys) in DMSO-d_6, and **c** PLGA-*b*-P(Lys) in D_2O

Micelle Characterization

Prepared micelles were characterized with dynamic light scattering, zeta potentiometer.

Micelles formed from PLGA-*b*-PLys showed a hydrodynamic average diameter of 144 nm with narrow distribution. The zeta potential of PLGA-*b*-P(Lys) micelles was measured as a function of pH. The highest value of the zeta potential was 57 mV at pH 3. Zeta potential was reduced with increasing pH up to 8.0 mV at pH 11. Positive values of the zeta potential in broad pH range indicated that an amine group of lysine units were protonated. Even at a high pH, micelles possessed a positive charge (Fig. 3). From these characterizations, it was confirmed that posi-

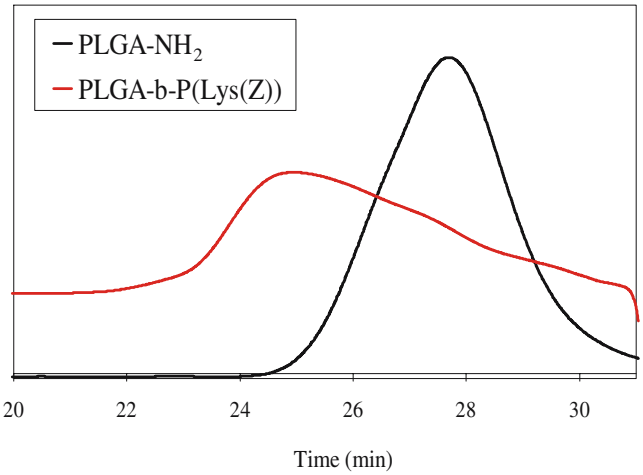

	M_n	M_w	PD
PLGA-NH_2	4400	7500	1.22
PLGA-b-P(Lys(Z))	22900	32500	1.42

Fig. 2 GPC chromatograms of PLGA homopolymer and PLGA-*b*-P(Lys(*Z*)) block polymer

tively charged PLGA-*b*-P(Lys) micelles were composed of the hydrophobic core of the PLGA block and the outer corona of the P(Lys) block with high charge density.

LbL Assembly

A schematic presentation of LbL micelle coating is shown in Scheme 2. Traditional LbL coating of polyelectrolytes is obtained by alternative layering of a polyelectrolyte layer and another polyelectrolyte with counterion. In the present study, positively charged micelles were used as a building block for LbL coating. Layer formation in situ was monitored by QCM to confirm the LbL deposition of positively charged PLGA-*b*-P(Lys) micelles. After deposition of an anionic polyelectrolyte layer, the cationic polymeric micelle solution at the concentration of 0.05 mg/ml was introduced to the substrate. Adsorption of micelles was monitored until the equilibrium was reached (Fig. 4). The first two pairs of polyelectrolytes were layered on the silicon crystal. Subsequent layering of cationic PLG-*b*-P(Lys) micelles came before an additional positive PAH layer (Fig. 4a) or anionic PSS layer (Fig. 4b). After an injection of cationic PLGA-*b*-P(Lys) micelle dispersion into the outmost PSS layer, the frequency decreased because of mass cumulated on the substrate. Simultaneously, dissipation increased until the frequency and dissipation curves reached a constant value of equilibrium in 1 h. In contrast, exposure of cationic PLGA-*b*-P(Lys) micelles to the outermost PAH layer did not cause significant frequency changes. These results showed that cationic PLGA-*b*-P(Lys) micelles were not significantly deposited on the outmost positive PAH layer, whereas PLGA-*b*-P(Lys) micelles were adsorbed on the negative PSS layer. Thus, it was proven that positively charged PLGA-*b*-P(Lys) micelles were truly deposited via electrostatic interaction.

QCM measures the mass balance of both micelles and water retained in the micelle vesicles. Rupturing of vesicles resulted in increase of frequency shift and decrease of mass because of escape of water from the vesicles. In the present study, increase in the frequency shift was not observed during the stabilization process of micelles. Frequency shifts were monotonically decreased, indicating continuous adsorption of polymeric micelles. This result indicated that cationic polymeric micelles were stable enough to be retained on the polyelectrolyte multiple layers, maintaining the micelle structure of the hydrophobic core and the hydrophilic corona.

After the deposition of the first micelle layer, a pair of intermediate polyelectrolyte layers (PAH/PSS) was appended before the second/multiple micelle layers were continued. After adsorption of the first micelle layer was equilibrated, anionic polymer (PSS) or cationic polymer (PAH) was exposed to the first micelle layer. The frequency shift increased with the injection of anionic PSS, showing that a portion of deposited micelles departed from the surface (Fig. 5c). Partial dissociation of the cationic micelle layer indicated that the surface charge was still negative even after the coating of positively charged micelles. The layered cationic micelles may be attracted to both negatively charged PSS in the

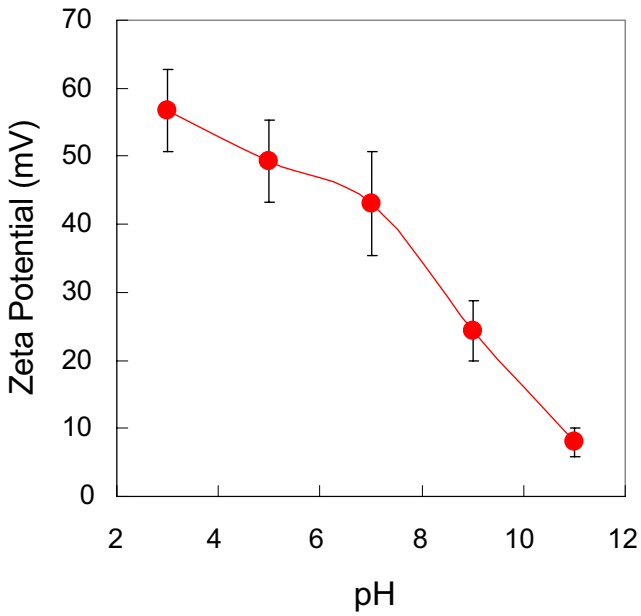

Fig. 3 Zeta potentials of PLGA-*b*-P(Lys) micelles as a function of pH

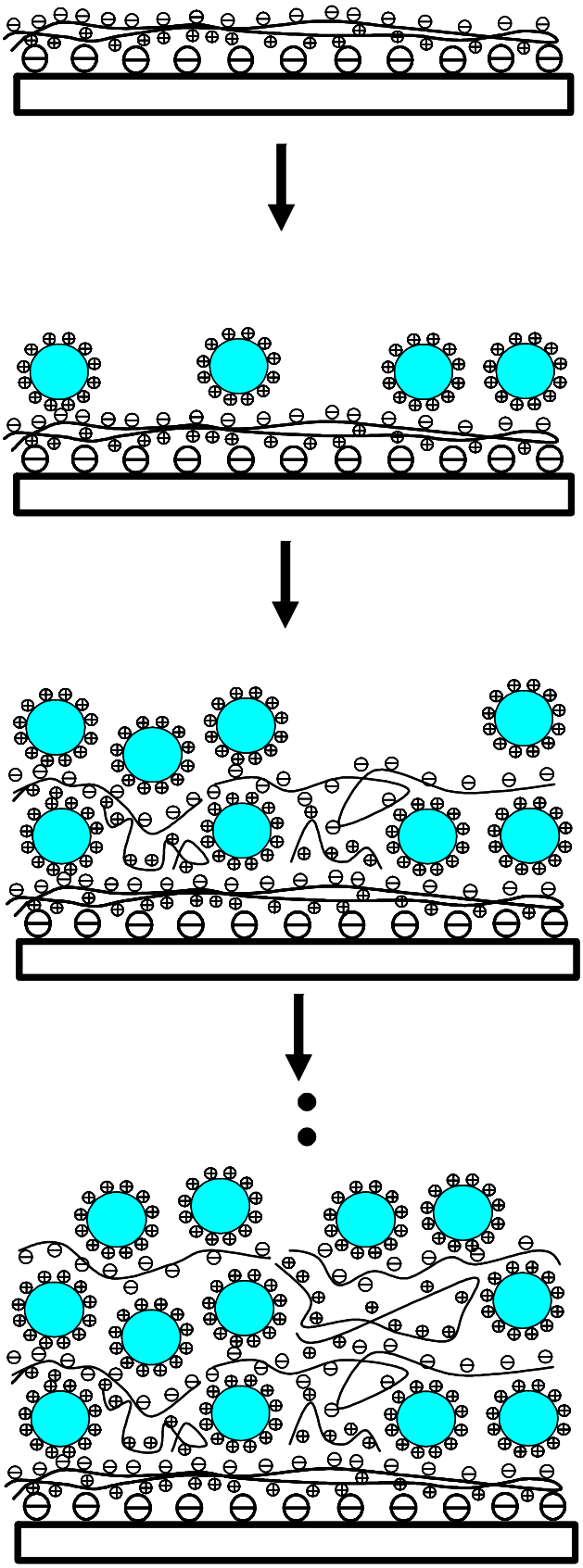

Scheme 2 Schematic illustration of LbL coating of cationic PLGA-*b*-P(Lys) micelles and polyelectrolytes

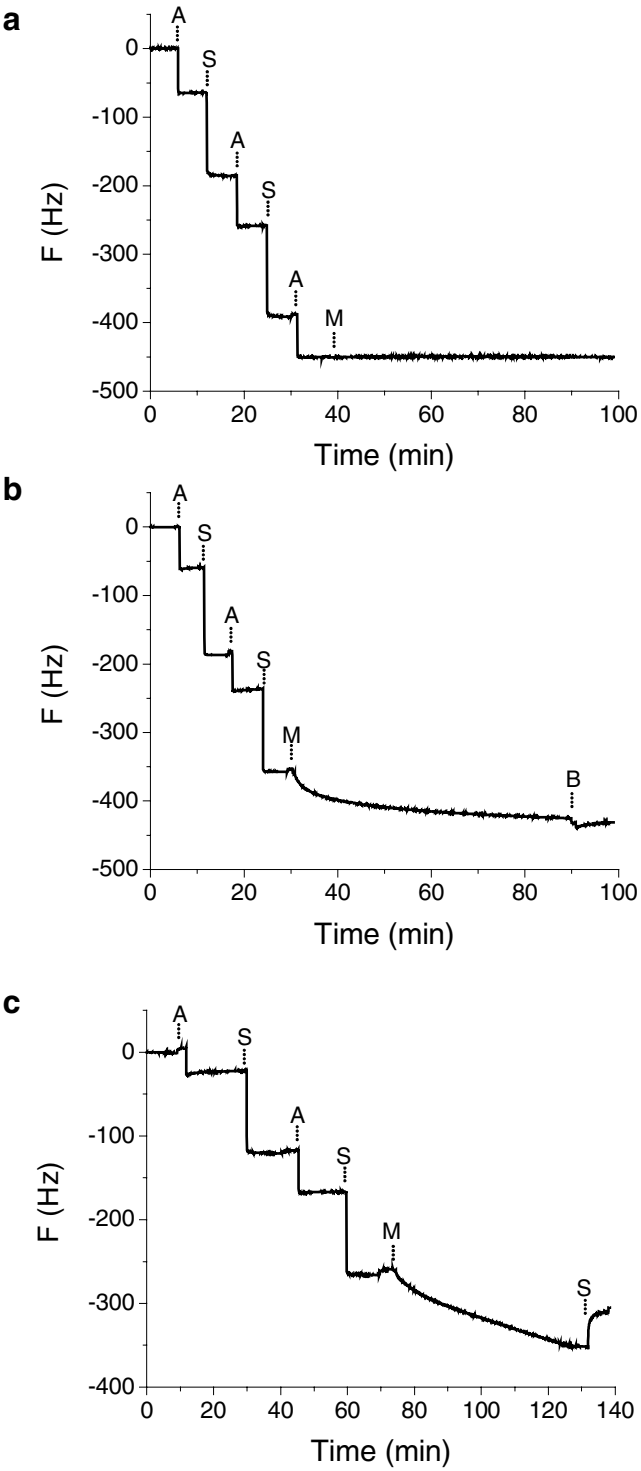

Fig. 4 Micelle layer formation in situ via electrostatic interaction monitored by QCM (A = PAH, S = PSS, M = micelles, B = buffer). Subsequent layering of cationic PLG-*b*-P(Lys) micelles before an additional positive PAH layer (**a**) or anionic PSS layer (**b**); frequency shift showing a portion of deposited micelles departing from the surface (**c**)

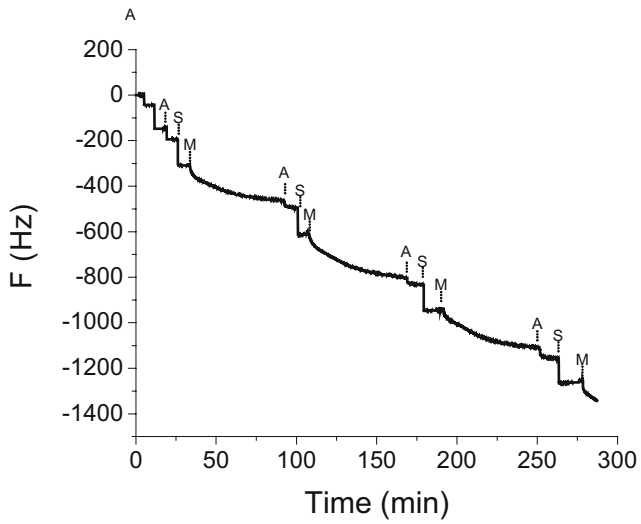

Fig. 5 In situ monitoring of micelle multiple layer formation via electrostatic interaction (A = PAH, S = PSS, M = micelles)

solution and the deposited PSS layer on the surface. In contrast, as positive PAH was introduced on the first micelle layer, the frequency shift decreased, showing that positive PAH was deposited even after cationic micelle adsorption (Fig. 5). Disassociation of cationic micelle from the surface did not occur after exposure to a solution of cationic PAH, indicating that subsequent PAH LbL coating was continued with the previously adsorbed micelle layers intact. Results infer that positively charged PLGA-*b*-P(Lys) micelles did not cover the entire surface area, but were immobilized on the surface as a vesicle form.

The PLGA-*b*-P(Lys) micelle multilayer was constructed by sequential deposition of *PAH*/*PSS*/*micelle layers* (Fig. 5). The intermediate layers between micelle layers were deposited with a pair of PAH/PSS. Four multiple micelle layers were deposited and monitored *in situ* (Fig. 5). A regular decrease in frequency shift was observed because of micelle deposition and the sequential deposition of a pair (PAH/PSS) between micelle layers.

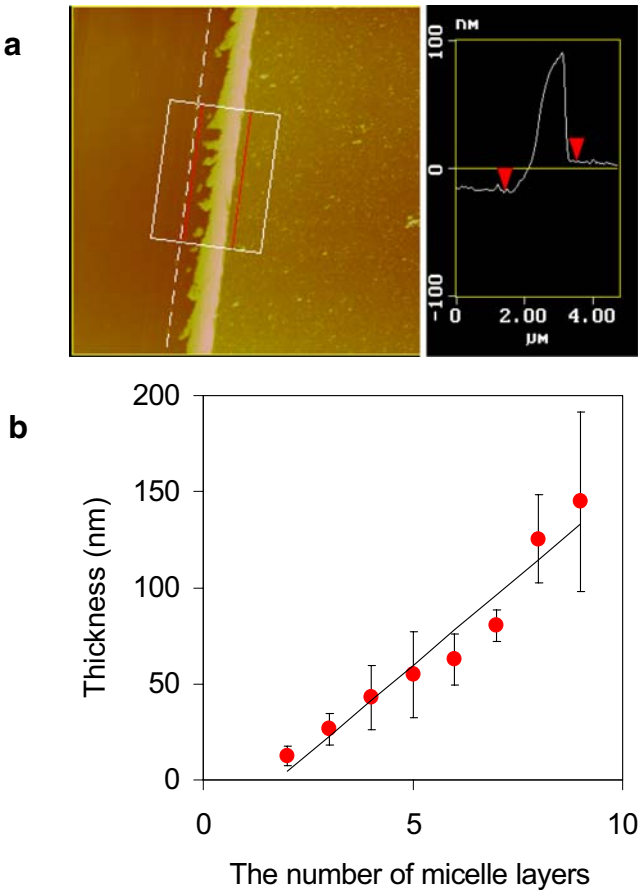

Fig. 7 The thickness growth of micelle layer. **a** The scratched film and height difference in marked area. **b** The growth of thickness as the increase of micelle layer

The extent of frequency decrease was approximately 80 Hz after each deposition of a micelle layer. The frequency change for each micelle layer was maintained the same. The same frequency change for each micelle layer indicated that the capability to build a layer via electrostatic force was recovered by additional intermediate deposition of a (PAH/PSS) layer. Continuous depositions of cationic PLGA-*b*-P(Lys) micelles and a pair of

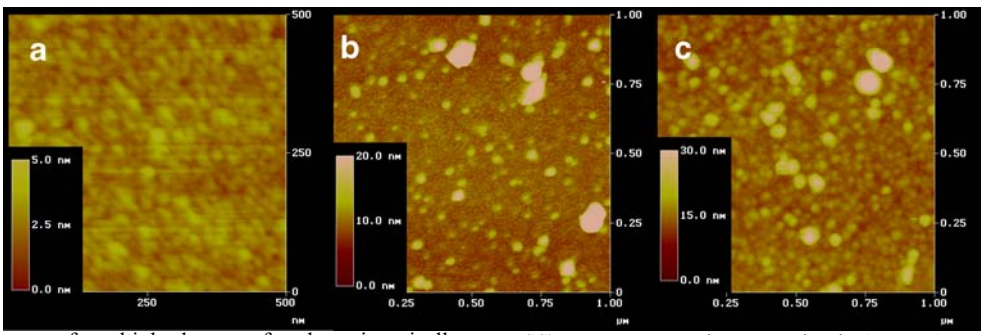

Fig. 6 AFM images of multiple layers of polymeric micelles. Subscript number represents the number of coating layer. **a** A pair of polyelectrolytes, $(PAA/PSS)_1$, as a control surface. Image size is 500×500×5 nm. **b** A pair of polyelectrolytes and a micelle layer, $(PAA/PSS)_2M$, were coated. Image size is 1 μm×1 μm×20 nm. **c** Three micelle layers, $(PAA/PSS)_4M_3$, were coated in sequence. Image size is 1 μm×1 μm×30 nm. AFM images were taken with the tapping mode

polyelectrolytes (PAA/PSS) showed that three-dimensionally constructed micelle assembly could be accomplished by the LbL method. Stable LbL deposition of micelles was monitored with QCM *in situ* for optimized layering.

Surface topology of the coated micelle layer was examined by atomic force microscope (AFM) *ex situ*. The micelle-coated substrates were lyophilized and imaged with AFM. The number of polyelectrolytes and micelle layers (n) was presented as the $((PAH/PSS)_{n+1}M)_n$. Figure 6a presents the control surface coated with a pair of polyelectrolytes $(PAH/PSS)_1$. The control surface was smooth and uniform without aggregation of polyelectrolytes. As the first micelle layer $((PAH/PSS)_2M)$ was coated on the substrate, the height increased from 5 to 20 nm, suggesting that micelles were deposited on the surface via electrostatic interaction (Fig. 6b). However, the entire surface was not fully covered with micelles. This result corresponded to the results that positive PAH was still deposited on the cationic micelle-coated layer as monitored by QCM. The dense third micelle layer $((PAH/PSS)_4M_3$, was evenly formed as shown in Fig. 6c. Images show that micelles were successfully coated on the surface between cationic PLGA-*b*-P(Lys) micelles and polyelectrolytes. The sizes of dried micelles on the layer ranged from 10 to 20 nm. The charged hydrophilic outer corona was flattened as it dried [31]. The micelle diameter measured from the AFM image was smaller than the hydrodynamic diameter.

The thickness of the micelle assembly was measured to examine the growth of three-dimensional multiple micelle layers. Coating of the micelle layers was repeated up to nine layers of micelles. A portion of the dried micelle-coated substrates was removed by scratching with a razor blade. Difference in height (i.e., thickness) at the edge was measured using the depth profile of an AFM image (Fig. 7a). The thickness increased as the number of micelle layers increased, as shown in Fig. 7b. The thickness of multiple micelle layers increased to 150 nm with nine micelle layers. Increase in the thickness showed that the architectural structure of the micelle layers was three-dimensionally constructed.

Conclusions

In the present study, PLGA-*b*-P(Lys) micelle with positively charged outer shells was prepared to use as a building block of LbL assembly. The three-dimensional LbL multilayers of PLGA-*b*-P(Lys) micelle were deposited on the surface via electrostatic interactions between cationic PLGA-*b*-P(Lys) micelles and the intermediate polyelectrolyte layer. Because PLGA-*b*-P(Lys) micelles can be used for delivery of poorly soluble drugs, LbL coating of PLGA-*b*-P(Lys) micelles can be a useful tool for deposition of many types of hydrophobic drugs and subsequent controlled release from various biomedical devices.

Acknowledgements This work is supported in part by NIH through grants GM065284 and HL78715.

References

1. Kabanov AV, Batrakova EV, Alakhov VY. J Control Release 2002;82:189–212.
2. Kataoka K, Kwon GS, Yokoyama M, Okano T, Sakurai Y. J Control Release 1993;24:119–132.
3. Kwon GS, Kataoka K. Adv Drug Deliv Rev 1995;16:295–309.
4. Otsuka H, Nagasaki Y, Kataoka K. Adv Drug Deliv Rev 2003;55:403–19.
5. Xu JP, Ji J, Chen WD, Shen JC. J Control Release 2005;107:502–12.
6. Zou JH, Zhao YB, Shi WF. J Phys Chem B 2006;110:2638–42.
7. Angelatos AS, Katagiri K, Caruso F. Soft Matter 2006;2:18–23.
8. Caruso F, Katagiri K. Am Chem Soc 2004;227:U546 (abstracts of papers).
9. Hammond PT. Adv Mater 2004;16:1271–93.
10. Hammond PT. Curr Opin Colloid Interface Sci 2004;4:430–42.
11. Katagiri K, Hamasaki R, Hashizume M, Ariga K, Kikuchi J. J Sol-Gel Sci Technol 2004;31:59–62.
12. Katagiri K, Hashizume M, Kikuchi J, Taketani Y, Murakami M. Colloids Surf B Biointerfaces 2004;38:149–53.
13. Michel A, Izquierdo A, Decher G, Voegel JC, Schaaf P, Ball V. Langmuir 2005;21:7854–59.
14. Michel M, Vautier D, Voegel JC, Schaaf P, Ball V. Langmuir 2004;20:4835–39.
15. Seantier B, Breffa C, Felix O, Decher G. J Phys Chem B 2005;109:21755–65.
16. Katagiri K, Caruso F. Macromolecules 2004;37:9947–53.
17. Michel M, Arntz Y, Fleith G, Toquant J, Haikel Y, Voegel JC, et al. Langmuir 2006;22:2358–64.
18. Emoto K, Iijima M, Nagasaki Y, Kataoka K. J Am Chem Soc 2000;122:2653–4.
19. Emoto K, Nagasaki Y, Kataoka K. Langmuir 1999;25:5212.
20. Emoto K, Nagasaki Y, Kataoka K. Langmuir 2000;16:5738–42.
21. Cho J, Hong J, Char K, Caruso F. J Am Chem Soc 2006;128:9935–42.
22. Huang N-P, Csucs G, Emoto K, Nagasaki Y, Kataoka K, Textor M, et al. Langmuir 2002;18:252.
23. Ma N, Wang Y, Wang Z, Zhang X. Langmuir 2006;22:3906–09.
24. Ma N, Zhang HY, Song B, Wang ZQ, Zhang X. Chem Mater 2005;17:5065–69.
25. Cheng H, de la Cruz MO. Macromolecules 2006;39:1961–70.
26. Jeong JH, Byun Y, Park TG. J Biomater Sci Polym Ed 2003;14:1–11.
27. Lavik EB, Hrkach JS, Lotan N, Nazarov R, Langer RA. J Biomed Mater Res 2001;58:291–94.
28. Daly WH, Poche D. Tetrahedron Lett 1988;29:5859–62.
29. Clark SL, Montague MF, Hammond PT. Macromolecules 1997;30:7237–44.
30. Marx KA. Biomacromolecules 2003;4:1099–120.
31. Talingting MR, Ma Y, Simmons C, Webber SE. Langmuir 2000;16:862–5.